

# A new automatic registration method for InSAR image based on multi-step strategy

**Bingqian Chen\***

*School of Environment Science and Spatial Informatics, China University of Mining and Technology, 1 Daxue Road, Xuzhou, 221116, China*

*Received 12 May 2014, www.tsi.lv*

---

## Abstract

Interferometric Synthetic Aperture Radar (InSAR) technology has been widely used in various applications. The registration of SAR (Synthetic Aperture Radar) images is the first step in interferometric processing therefore accurate registration is essential for the successful creation and interpretation of interferometric products. However, with the growing number of SAR satellite launch and the amount of data acquisition, the degree of automation of image registration have become increasingly demanding. In this paper, we propose an automatic registration approach based on multi-step matching strategy. In the first step, key points are detected and matched using modified scale invariant feature transform (SIFT) operator which modified by us reducing the influence of speckles. In this step, owing to the existing of speckle and the defect of matching strategy of SIFT operator, the expected level of matching accuracy is about 2 to 3 pixels. In the second step, correlation matching (CM) is used to exclude the matched points with low correlation. In the third step, the probability relaxation (PR) algorithm based on global matching is used to induce consistency constraint and ensure reliability of the matching result. Finally, corresponding transformation function is determined through the relationship established by matched point pairs. In order to verify the applicability of proposed methodology, two SAR images acquired over mountainous regions are used in our experiment. The experiment results show that subpixel registration accuracy and good efficiency have been achieved, which demonstrates the correctness and feasibility of proposed method.

*Keywords:* InSAR, Image registration, Feature detection, SIFT, Correlation matching

---

## 1 Introduction

InSAR is a technology developed in recent decades, which utilizes the relationship between the phase difference and spatial distance difference of complex data obtained in two repeat observations to extract three-dimensional information or elevation change information of ground surface [1, 2]. Due to its outstanding advantages of fast, high-precision, all-time, all-weather and large areas, it has been used in many domains, like Digital Elevation Model (DEM) generation[3], target recognition [4], volcano activity detection [5], landslide movements studies [6], and many more [7-9]. Prior to most of mentioned applications, SAR images are required to be aligned accurately (usually subpixel level).

The definition of the image registration can be explained as two images obtained from different time, sensors, or perspectives are unified to the same coordinate system according to certain criterion. In general, most image registration methods consist of three main steps: locating of GCPs (Ground Control Points), matching of GCPs, determining of geometrical transformation function. Some obvious ground objects can be used as GCPs, like buildings, bridges, crossroads, etc. The identification of sufficient GCPs pairs allows the transformation function to be determined. Finding suitable GCPs pairs is the most difficult step.

Traditional registration method makes use of GCPs determined by operating staff, which is time-consuming and imprecision and is practically impossible for single look complex (SLC) SAR data. Therefore, many researchers have focused on the study of automatic registration method [10-11]. However, the complexity of registration of SAR image is much higher than optical image due to the existing of speckle noise and blur-texture feature.

In our study, we introduce feature-based scale invariant feature transform (SIFT) operator to extract prominent features points and complete initial registration, then area-based correlation matching (CM) is used to exclude the matched points with low correlation, to achieve the effect of removing of mismatch points. Furthermore, the probability relaxation (PR) technique based on global matching algorithm is used to induce consistency constraint and ensure reliability of the matching result. Finally, the parameters of transformation function are computed through the established key point correspondence, and slave image is transformed through the transformation function. The proposed method is an automatic approach using a multistep matching strategy, which completes the registration procedure from coarse to fine precision. The results of the experiment are promising in their reliability, accuracy, and computing efficiency, which prove the feasibility of proposed method.

---

\* *Corresponding author* e-mail: bqccumt@gmail.com

## 2 Methodology

Our method mainly contains four steps. The matching accuracy of key points is improved through the first three steps, moving one-step at a time, coarse to fine, thus an accurate mapping function model is established through the fourth step. The flowchart of the main steps of proposed method is illustrated in Figure 1. In the first step, key points are detected and matched using modified SIFT operator. In this step, due to the existing of speckle and the defect of matching strategy of SIFT operator, the expected level of matching accuracy is about 2 to 3 pixels. In the second step, CM is used to exclude the matched points with low correlation, to achieve the effect of removing of mismatch points. In the third step, the PR technique based on global matching algorithm is used to induce consistency constraint and ensure reliability of the matching result. Finally, the parameters of transformation function are computed through the established key point correspondence, and slave image is transformed by means of the transformation function. Although the slave images are SLC data, the whole procedure processed intensity images or power-detected images, i.e., it avoided computing the complex data.

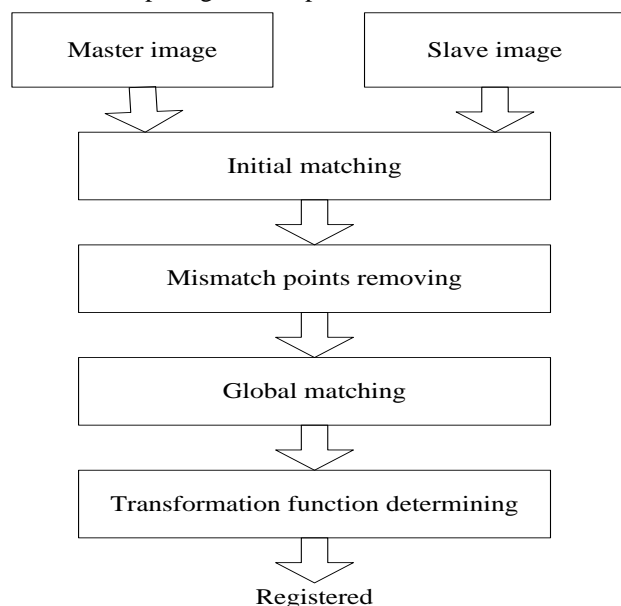


FIGURE 1 Flowchart of the main steps of proposed model

### 2.1. INITIAL MATCHING

#### 2.2.1 Key points detection

The entire process flow of proposed method starts from key point detection. For this purpose, the first step is to establish the image scale space. For a two-dimensional

image, its corresponding scale space  $L(x, y, \sigma)$  can be obtained by convolving the image with Gaussian kernel:

$$L(x, y, \sigma) = G(x, y, \sigma) * I(x, y), \quad (1)$$

where  $I(x, y)$  represents the two-dimensional image coordinate,  $G(x, y, \sigma)$  represents the Gaussian kernel,  $\sigma$  represents the variance of the Gaussian distribution. In order to detect key points efficiently in the scale space, difference of Gaussians (DoG) scale space  $D(x, y, \sigma)$  is created by means of convolving the image with different scale space Gaussian kernels in the second step, and DoG scale space is defined as:

$$D(x, y, \sigma) = (G(x, y, k\sigma) - G(x, y, \sigma)) * I(x, y) = L(x, y, k\sigma) - L(x, y, \sigma), \quad (2)$$

where  $k$  is the scale difference factor. Finally, the extrema are obtained through comparing the value of DOG of sample pixel with its surrounding eight pixels in the same scale space and the eighteen pixels in adjacent upper and lower scale space, respectively. If the value of sample pixel is larger or smaller than other neighbours, it will be accepted as an initial key point.

Here considering the requirement of computational efficiency and the influence of speckle noise, the original algorithm of key point detection is adapted which skip the searching for key points in first octave of the scale-space pyramid. This modification is called SIFT-OCT, more details about SIFT-OCT can be found in literature [12].

#### 2.1.2 Key Points Matching

According to the original matching strategy of SIFT operator proposed by Lowe [13], the smallest Euclidean distance criterion is adopted as similarity index, in other words, if the distance between two descriptor vectors defined by SIFT operator are smaller than others, corresponding points are taken as a matching pair. In our initial matching process, the strategy of smallest Euclidean distance is adopted. However, the quality of matching result using simple distance matching strategy is poor and cannot satisfy our requirement of accurate registration. An example of original SIFT operator matching result is illustrated in Figure 2. As shown in Figure 2, the positions of dots in the left image correspond to the position of dots in the right image and mismatch situations happening in the same colour rectangle frame, which will affect the final accuracy of image registration, therefore, in the following steps, the matched pairs will be refined by CM and Global image matching.

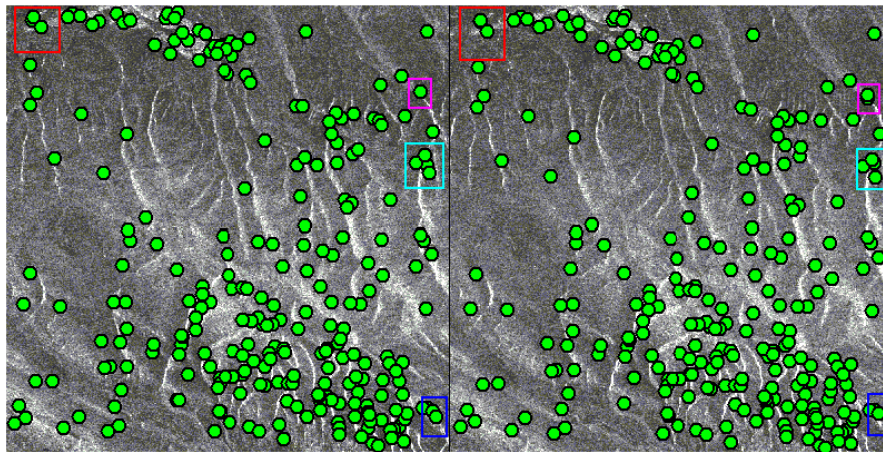


FIGURE 2 The matching result by original SIFT operator

### 2.2 MISMATCH POINTS REMOVING

Area-based CM methods also called template matching [14]. A certain number of feature points are firstly selected based on some kind algorithm (e.g. SIFT operator) in the master image, and then a certain size window with the feature point centred is determined, and the window moves on the slave image pixel by pixel to search the window with high set correlation. Finally, the central pixels of the two windows with highest correlation are considered as the matching points. Generally speaking, the conventional CM methods include correlation coefficient method, Fourier method and mutual information method. Nevertheless, the calculation of the mentioned methods is complex especially when deal with large images. Because we have already obtained initial matching point pairs by SIFT operator in section 2.1 and our ultimate purpose of the study is the removing of mismatch points ,therefore, a search in all over the image is unnecessary we can calculate the correlation value of the matched points directly and judge whether it meet the requirement of threshold value. If not, these points will be removed.

Correlation coefficient, is originally defined by complex calculation and now is defined by us just calculating intensity value, which avoids computing the complex data thus computational efficiency is improved. Here, correlation coefficient is defined as follows:

$$\rho = \frac{\sum_{m=1}^k \sum_{n=1}^g R(m, n)S(m, n)}{\sqrt{\sum_{m=1}^k \sum_{n=1}^g R(m, n)^2} \sqrt{\sum_{m=1}^k \sum_{n=1}^g S(m, n)^2}}, \quad (3)$$

where  $\rho$  is the correlation coefficient (between 0 and 1),  $R(m, n)$  and  $S(m, n)$  represent the coordinate of certain matched point in master image and the corresponding coordinate of point in slave image, respectively. The matching window size is  $k \times g$ . The detailed implementation steps of CM are described as follows:

(i) The acquirement of initial matching points: The initial matching points are obtained by modified SIFT operator, as mentioned in section 2.1. We can assume set  $R' = \{R_1', R_2', \dots, R_i'\}$  is initial matching points in the master image and  $S' = \{S_1', S_2', \dots, S_i'\}$  is the corresponding matching points in the slave image, respectively.

(ii) The calculation of correlation coefficient: The value of correlation coefficient of the matched points is calculated according to equation (3), and a certain size search window is needed in the calculation processing of correlation coefficient. From section 2.1 we can know that the extrema are detected in the DoG scale space by comparing every pixel to the eight neighbouring pixels in the same scale space, therefore, we can choose the range of  $3 \times 3$  as our size of search window.

(iii) The judgement of correlation coefficient: If the correlation coefficient  $\rho$  is greater than threshold  $Y$ , it is accepted as right matched points and retained, otherwise excluded. Here 0.3 is adopted as the threshold  $Y$  in our experiments.

Some obvious mismatch points can be removed by CM, and the number of initial matching points also can be lessened to a certain extent by adjusting the threshold value of correlation coefficient, which will reduce the amount of calculation of next steps. However, CM belongs to isolated single point matching and does not take account of the compatibility of the matching result of one point pair with its neighbours, which leads to the uncertainty existing of matching result and false matches may still occur. Therefore, PR algorithm based on global matching is introduced in the next step.

### 2.3 GLOBAL MATCHING

In this section, the PR algorithm is adopted to further refine and ensure reliability of the matching result obtained in section 2.2. PR algorithm was firstly used for image registration by Rosenfeld et al. in 1976 [15]. The PR algorithm is a parallel and iterative computation process. Every point on the processing is in parallel in every iteration process, and the iteration results of the

point are adjusted by means of the result of surrounding points in next iteration. This parallel iterative process not only taken into account the impact on the surrounding results, but also has the characteristics of parallel processing, therefore, it has been widely used in various fields. In our study, the PR algorithm is used and two matched point sets obtained in section 2.2 are regarded "object" and "class", respectively. Therefore, the problem from registration converts into classification. The detailed process is described as follows.

Since we have acquired preliminary matching point pairs in section 2.2, here we assume matched points set  $T = \{T_1, T_2, \dots, T_j\}$  as "object" set and correspondign set  $S = \{S_1, S_2, \dots, S_i\}$  as "class" set. As shown in Figure 3, pixel  $m$  is the "object" in the master image, pixel  $n$  is the corresponding "class" in the slave image. And now the image matching become solving the problem  $T_m \in S_n$ . To improve the reliability of result of classification, the global consistency must be considered, i.e. classification results are in harmony with each other. Therefore, on the basis of the requirement of PR algorithm, the probability  $P_{mn}$  of  $T_m \in S_n$  and the compatible coefficient  $C(m, n; t, g)$  of  $T_m \in S_n \cap T_t \in S_g$  should be determined firstly.

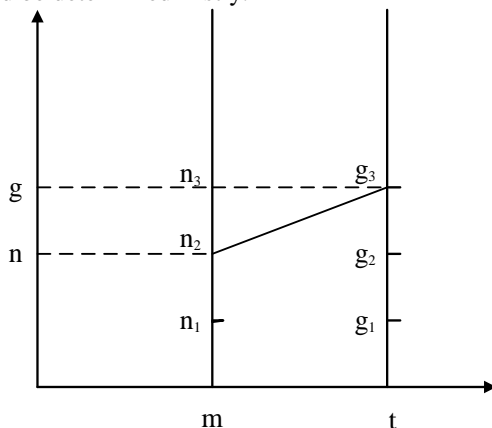


FIGURE 3 PR algorithm with bridge model

Because the coherence of matched point pairs are calculated by CM algorithm in section 2.2, here we take the correlation coefficient  $\rho_{mn}$  as the initial value  $P_{mn}$  of  $T_m \in S_n$ , and also we define the correlation coefficient  $\rho(\bar{m}, \bar{t}; \bar{n}, \bar{g})$  between interval  $[m, t]$  and  $[n, g]$  (Figure 3) as the initial compatible coefficient  $C(m, n; t, g)$  of  $T_m \in S_n \cap T_t \in S_g$ , i.e.,

$$C(m, n; t, g) \propto \rho(\bar{m}, \bar{t}; \bar{n}, \bar{g}). \tag{4}$$

While the initial measurement of  $P_{mn}$  and  $C(m, n; t, g)$  are determined, the relaxation iterative procedure can be conducted according to the following equations:

$$Q(m, n) = \sum_{t=1}^{j(M)} \left( \sum_{g=1}^{i(N)} C(m, n; t, g) P(m, n) \right) \tag{5}$$

$$P^{(u)}(m, n) = \frac{P^{(u-1)}(m, n)(1 + IQ(m, n))}{\sum_{n=0}^{i(F)} P^{(u)}(m, n)}$$

where  $j(M)$  represents the number of neighbor points of point  $m$ ,  $i(N)$  and  $i(F)$  represent the number of candidate matching points of slave image,  $u$  is the ordinal number of iteration,  $I$  represents the incremental coefficient. Iteration termination condition of equation 5 is defined as:

$$|P^{(u)}(m, n) - P^{(u-1)}(m, n)| \leq \epsilon. \tag{6}$$

### 3 Evaluation of Proposed Model Performance

To evaluate the performance of proposed model, several criteria are introduced and described as follows:

(i) Running time: For testing the operating efficiency of proposed method, we recorded the turnaround time, which includes the time for the detection and execution of the matching process.

(ii) Standard deviations (STDs): To assess the performance and verify the feasibility of the proposed method, the STDs are introduced as an indicator of measuring the accuracy of the registration. The STDs computing formula is defined as follows:

$$\left\{ \begin{aligned} STD_{range} &= \sqrt{\frac{\sum_{i=1}^n (x_i - x'_i)^2}{n-1}}, \\ STD_{azimuth} &= \sqrt{\frac{\sum_{i=1}^n (y_i - y'_i)^2}{n-1}} \end{aligned} \right. \tag{7}$$

where the  $(x_i, y_i)$  represents the coordinate of pixel  $i$  in master image,  $(x'_i, y'_i)$  represents the coordinate of the same object in the transformed slave image,  $n$  is the number of matched point pairs.

(iii) Interferogram quality evaluation: Interferogram is the product obtained by complex conjugate multiplying of two registered images, and its fringes definition is taken as the criterion of registration quality by many researchers [16]. That is, if the interferometric fringes are clear, it indicates a good registration result is achieved. However, it is a sufficient condition, not a necessary condition, i.e. although clear interferometric fringes indicate a good quality of registration, the blurred fringes in interferogram not always mean poor registration accuracy because the quality of interferogram depends on not only registration but also temporal baseline, spatial baseline and noise. Here the quality of an interferogram is only used as qualitative description of registration results.



(iv) Coherence estimation: Coherence is an important concept in the InSAR technology, which indicates the degree of similarity between the two SAR images. The coherence value is not only an important evaluation criterion for the quality of local interferometric fringes, but also a necessary condition to guarantee the reliability of the results [17]. In our study, the mean value and corresponding STDs of coherence are used to verify the reliability of registration result. Here the coherence value  $\gamma(0 < \gamma < 1)$  is defined as follows:

$$\gamma = \frac{|E[f_1 \cdot f_2^*]|}{\sqrt{E[|f_1|^2]E[|f_2|^2]}}$$
(8)

where  $f_1$  and  $f_2$  represent the two registered SAR images.

### 4 Experiments and Results

#### 4.1 DATASET

To verify the feasibility of the proposed method, two images (size 600×600 pixel) acquired by X-band TerraSAR-X satellite (launched by Deutsches Zentrum für Luft- und Raumfahrt in 2007) are used in our first experiment. The images were acquired over Van, Turkey, featuring a mountain land cover class. From Table 1 we can know that the time difference between two images is eleven days.

TABLE 1 Details of TerraSAR-X images

Image	TerraSAR-X (Master image)	TerraSAR-X (Slave image)
Mode	Stripmap Mode	Stripmap Mode
Pixel Spacing (m)	3	3
Incidence Angle	33.18°	33.18°
Date of Acquisition	31/10/2011	11/11/2011
Wavelength (cm)	3.1	

#### 4.2 EXPERIMENT RESULTS

The matching results using proposed method in different steps are seen in Figure 5(a), (b), and (c). The number of initial key points detected by modified SIFT operator is 2266 in the master image and 1951 in the corresponding slave image (Table 2). After applying of SIFT matching strategy 264 matching point pairs are obtained. In this step, owing to the speckle existing and the defect of matching strategy of SIFT operator, mismatch occasions may occur (Figure 4(a)), which lead to the high STDs in range and azimuth directions (Table 2). So in the next steps, CM and PR matching are adopted to refine the matched pairs, the matching results are seen in Figure 4(b) and (c), respectively. From Figure 4(b) we can know that the quality of matched points is improved but still mismatching cases happening. Figure 4(c) shows that the occasions of mismatching are disappeared and the final

number of matching point is reduced to 75 and the corresponding STDs are subpixel in both range and azimuth directions (Table 2). The improvement in the STDs show that initial matching by SIFT operator and CM provides reliable initial locations.

To further examine the effect of image registration, an interferogram (Figure 5) is produced by a point-wise complex conjugate multiplication of corresponding pixels in master image and registered image. And also, corresponding coherence map (Figure 6) is obtained by calculating equation 8.

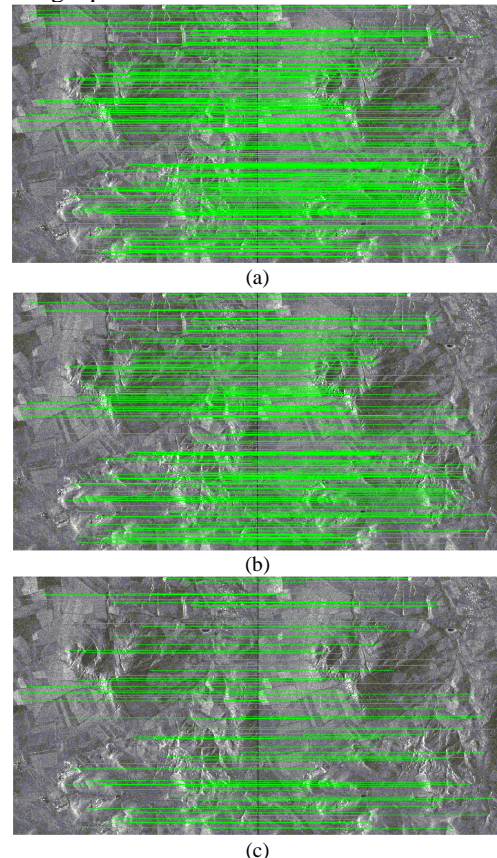


FIGURE 4 Matching results in different steps. (a) Matching result using the SIFT operator. (b) Matching result after using CM to (a). (c) Matching result after using PR matching to (b)

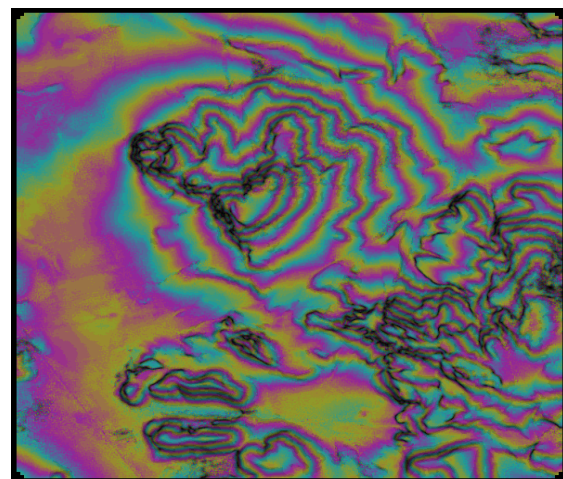


FIGURE 5 Interferometric fringes (Van, Turkey) of X-band images

By visual inspection, we can find that most of the interferometric fringes are clear and continuous, which indicates the good quality of interferogram (Figure 5), and corresponding a good coherence map (Figure 6(a), high coherence is found in bright areas and low coherence in dark areas.). In order to describe the value of coherence quantitatively, the histogram of coherence image is introduced (Figure 6(b)) and the mean of the

distribution and corresponding STDs are used to coherence estimation. In Figure 6(b), the mean is 0.8395, while its STDs is 0.0454. Both the high quality of interferogram and coherence map also proves the good result of registration. And also from Table 2 it can be observed that the process speed of the test data is near real time and sufficient for our work requirement.

TABLE 2 Experimental results for TerraSAR-X images

Matching Algorithm	SIFT	SIFT + CM	SIFT+CM+PR
Number of key points	Ref:2266 Inp:1951	Ref:264 Inp:264	Ref:191 Inp:191
Number of matches	264	191	75
STDs (pixel)	Range:2.605 Azimuth:2.413	Range:1.217 Azimuth:1.130	Range:0.0504 Azimuth:0.0717
Turnaround time (s)		13	

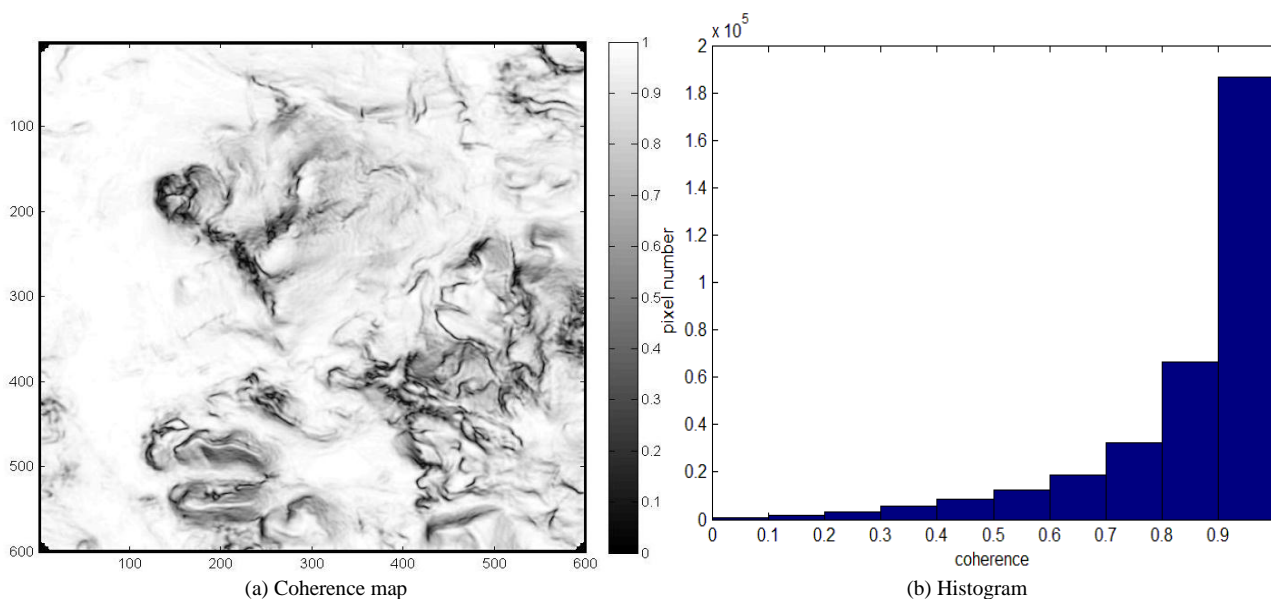


FIGURE 6 Coherence map and the corresponding histogram of coherence

### 5 Conclusions

In this paper, we present a novel SAR image registration method based on multi-step, which completes the registration procedure from coarse to fine precision. The feature-based SIFT operator is firstly introduced to extract prominent features points and complete initial matching, then area-based CM is used to exclude the matched points with low correlation, to achieve the effect of removing of mismatch points. Finally, the PR algorithm based on global matching is used to induce consistency constraint and ensure reliability of the matching result. The proposed method is an automatic approach which completes the entire registration procedure without manual intervention.

We conduct one experiment using the proposed method, and make a detailed analysis to the experiment results in many aspects, i.e. key point detection, quality of interferogram and coherence map, matching accuracy and process turn around time. The experiment results

show that the proposed methodology shows robust performance and subpixel registration accuracy can be achieved. The experiments results have also shown the process speed of the test data is near real time, which indicate the process efficiency can be guaranteed for larger images. Moreover, another advantage of our method is that it does not require special filtering process before the SAR image registration.

### Acknowledgments

This work is funded by the natural science foundation of china (No.41071273 and No. 41272389), a project funded by the priority academic program development of Jiangsu Higher Education Institutions (No.SZBF2011-6-B35), A project of graduate research and innovation of ordinary university in Jiangsu Province (No.CXZZ13\_0936). Relevant radar data were provided by the German Aerospace Centre TerraSAR-X Science Plan (LAN1425).

## References

- [1] Ouchi K 2013 *Remote Sens.* **5** 716-807
- [2] Burgmann R, Rosen P A, Fielding E J 2000 *Annu. Rev. Earth Planet. Sci.* **28**(1) 169-209
- [3] Ortiz S M, Breidenbach J, Knuth R, Kändler G 2012 *Remote Sens.* **4**(3) 661-81
- [4] Huan R H, Pan Y 2013 *Prog. Electromagn. Res.* **134** 267-88
- [5] Papageorgiou E, Fomel M, Parcharidis I 2012 *IEEE J-STARS.* **5**(5) 1531-7
- [6] Liu P, Li Z H, Hoey T, Kincal C, Zhang J F, Zeng Q M, Muller J P 2013 *Int. J. Appl. Earth Obs. Geoinf.* **21** 253-64
- [7] Kobayashi S, Omura Y, Sanga-Ngoie K, Widyorini R, Kawai S, Supriadi B, Yamaguchi Y 2012 *Remote Sens.* **4**(10) 3058-77
- [8] Pivot C F 2012 *Remote Sens.* **4**(7) 2133-55
- [9] Gama F F, Santos J R D, Mura J C 2010 *Remote Sens.* **2**(4) 939-56
- [10] Bradley P E, Jutzi B 2011 *Remote Sens.* **3**(9) 2076-88
- [11] Ben-Dor E, Brook A 2011 *Remote Sens.* **3**(1) 65-82
- [12] Schwind P, Suri S, Reinartz P, Siebert A 2010 *Int. J. Remote Sens.* **31**(8) 1959-80
- [13] Lowe D G 1999 Object recognition from local scale-invariant features *In Processing of International Conference on Computer Vision (Corfu, Greece)* 1150-57
- [14] Chen J H, Chen C S, Chen Y S 2003 *IEEE Trans. Signal Process.* **51**(1) 230-43
- [15] Rosenfeld A, Hummel R A, Zueker S W 1976 *IEEE Trans. Syst. Man Cybern.* **SMC-6** 420-33
- [16] Eldhuset K, Aanvik F, Aksnes K 1996 *First results from ERS tandem InSAR processing on Svalbard* <http://www.geo.unizh.ch/rsl/fringe96/papers/eldhuset-et-al/> (accessed 8 January 2008).
- [17] Gens R 1998 *Quality assessment of SAR interferometric data* Hanover University: Hanover, Germany

## Authors



**Bingqian Chen, born on September 24, 1986, China**

**University studies:** Doctoral candidate

**Scientific interest:** His research interests include radar data processing, optimization algorithms, data fusion, and use of remote sensing information for Civil Protection applications.

**Experience:** Bingqian Chen was born in Henan Province, China. He received the B.S. degree in surveying and mapping engineering at the Henan Polytechnic University in June 2010. He has been studying the postgraduate program for Doctor degree on Geodesy and Surveying Engineering in the School of Environment Science & Spatial Informatics at China University of Mining & Technology since September, 2012.